

Dimensional Stability of Additively Manufactured Diagnostic Maxillary Casts Fabricated with Different Model Resins

Mustafa Borga Dönmez, DDS, PhD

Department of Prosthodontics, Faculty of Dentistry, Istinye University, Istanbul, Turkey; Department of Reconstructive Dentistry and Gerodontology, School of Dental Medicine, University of Bern, Bern, Switzerland.

Alena Bruna Wepfer, Med dent

Department of Reconstructive Dentistry and Gerodontology, School of Dental Medicine, University of Bern, Bern, Switzerland; Private practice, Bern, Switzerland.

Mehmet Esad Güven, DDS, PhD

Department of Prosthodontics, Faculty of Dentistry, Necmettin Erbakan University, Istanbul, Turkey.

Gülce Çakmak, DDS, PhD

Department of Reconstructive Dentistry and Gerodontology, School of Dental Medicine, University of Bern, Bern, Switzerland.

Martin Schimmel, MAS, Prof Dr med dent

Department of Reconstructive Dentistry and Gerodontology, School of Dental Medicine, University of Bern, Bern, Switzerland; Division of Gerodontology and Removable Prosthodontics, University Clinics of Dental Medicine, University of Geneva, Geneva, Switzerland.

Burak Yilmaz, DDS, PhD

Department of Reconstructive Dentistry and Gerodontology and Department of Restorative, Preventive and Pediatric Dentistry, School of Dental Medicine, University of Bern, Bern, Switzerland; Division of Restorative and Prosthetic Dentistry, The Ohio State University College of Dentistry, Columbus, Ohio, USA.

Purpose: To evaluate the effect of model resin type and time interval on the dimensional stability of additively manufactured diagnostic casts. **Materials and Methods:** Ten irreversible hydrocolloid impressions and 10 impressions from an intraoral scanner were made from a reference maxillary stone cast, which was also digitized with a laboratory scanner. Conventional impressions were poured in type III stone (SC), while digital impressions were used to additively manufacture casts with a nanographene-reinforced model resin (GP) or a model resin (DM). All casts were digitized with the same laboratory scanner 1 day (T0), 1 week (T1), 2 weeks (T2), 3 weeks (T3), and 4 weeks (T4) after fabrication. Cast scans were superimposed over the reference cast scan to evaluate dimensional stability. Data were analyzed with Bonferroni-corrected repeated measures ANOVA ($\alpha = .05$). **Results:** The interaction between the main factors (material type and time interval) affected anterior teeth deviations, while the individual main factors affected anterior teeth and entire-cast deviations ($P \leq .008$). Within anterior teeth, DM had the lowest deviations at T3, and GP mostly had lower values at T2 and lower deviations at T3 than at T0 ($P \leq .041$). SC had the highest pooled anterior teeth deviations, and GP had the highest pooled entire cast deviations ($P < .001$). T3 had lower pooled anterior teeth deviations than at T0, T1, and T4, and higher pooled entire cast deviations than T1 were demonstrated ($P \leq .027$). **Conclusions:** The trueness of nanographene-reinforced casts was either similar to or higher than that of other casts. Dimensional changes were acceptable during the course of 1 month. *Int J Prosthodont* 2024;37(suppl):s119–s126. doi: 10.11607/ijp.8877

A complete digital workflow has become a viable option due to the advancements in CAD/CAM technologies,¹ as digitization of a patient's intraoral situation via an intraoral scanner (IOS) has eliminated many disadvantages of conventional impressions^{2,3} and physical models.^{4,5} However, it is still possible to fabricate a physical cast from the scan data using either subtractive or additive manufacturing technologies.^{6,7} Additive manufacturing is becoming an indispensable part of

Correspondence to:
Dr Mustafa Borga Dönmez,
mustafa-borga.doenmez@unibe.ch

Submitted November 15, 2023;
accepted November 20, 2023.
©2024 by Quintessence
Publishing Co Inc.

dentistry, as this layer-by-layer construction enables the fabrication of dental casts for diagnostic and treatment purposes.^{2,8,9} Among different additive manufacturing technologies,^{9–12} digital light processing (DLP) has been commonly used in dentistry as it reduces fabrication time and detailed objects can be manufactured with smooth surfaces.^{13,14}

Fabrication trueness of additively manufactured (AM) dental workpieces was reported to be affected by several factors, one of which is the resin used.¹⁵ Recently, a nanographene-reinforced dental model resin (G-Print, Graphenano Dental) has been introduced to create smooth and pore-free printed casts with high dimensional stability.¹⁶ Graphene is an allotrope of carbon that has a unique honeycomb-shaped two-dimensional structure,¹⁷ which allows its use as a reinforcing agent in polymers.¹⁸ Reinforced model resin use may be advantageous for improved dimensional stability considering the potential wear of surfaces, particularly during articulation and over time. However, to the present authors' knowledge, no study has evaluated this model resin. Previous promising findings on the mechanical and optical properties of subtractively manufactured nanographene-reinforced polymers^{17–24} encourage the investigation of the different properties of AM versions of these resins when used for model fabrication.

Regardless of the manufacturing method, a dental cast should replicate the intraoral situation as accurately as possible and have adequate dimensional stability over time. Even though there are studies on the fabrication trueness of AM dental casts,^{5,7,8,11,12,14,25–27} the number of studies on the dimensional stability of these casts is limited.^{1,6} In addition, those studies on the dimensional stability of AM casts did not involve comparisons with stone casts.^{1,6} Therefore, the purpose of the present study was to evaluate the dimensional stability of AM diagnostic casts fabricated using two different model resins and compare it to those of a stone cast every week over 4 weeks. The null hypothesis was that the material type and time interval would not affect the dimensional stability of dentate maxillary casts within different regions of the casts.

MATERIALS AND METHODS

A priori power analysis (power = 90%, $f = 1.99$, $\alpha = .05$) based on the results of a previous study¹ on the stability of AM dentate casts deemed nine specimens per group sufficient. To increase the statistical power, 10 specimens were planned to be fabricated. A dentate maxillary master stone cast was digitized using a laboratory scanner (E4 Dental Scanner, 3Shape) with 4- μm accuracy, and its standard tessellation language (STL) file was saved as the master cast STL (MC-STL) file to be used in deviation analyses. Then, a single operator (A.B.W.)

made 10 conventional impressions of the master cast by using irreversible hydrocolloid (Alginoplast, Heraeus Kulzer) that was prepared with a ratio of 40 g of powder to 88 mL water at room temperature, and stock impression trays (Disposable Impression Trays, 3M ESPE) were used to fabricate stone casts (SCs). The master cast was soaked in water in between each impression. Each impression was then poured in type III stone (Zeta Selenor Extra Export, Industria Zingardi) that was prepared with 25 mL of osmosis water per 100 g of hard dental stone. The stone was first mixed by hand for 30 seconds and then under vacuum for 60 seconds. A regular plastic cast base was also used while preparing the casts. All impression and pouring procedures were performed at room temperature on the same day.

The same operator digitized the master cast 10 times using an IOS (CEREC Primescan version 5.2, Dentsply Sirona) the next day. The manufacturer's recommended pattern of scanning was followed, beginning with palatal, occlusal, and buccal surfaces and finishing the scan with S-shaped movements in the palate.²⁸ The IOS was calibrated before each scan, and all scans were performed in a humidity- and temperature-controlled room with daylight. STL files of IOS master cast scans were imported into a nesting software (Composer version 1.3, Asiga), and each STL file was positioned with its base parallel to the build platform. Support structures were generated automatically, and solid casts were fabricated using either a dental model resin (DM; DentaModel, Asiga) or a nanographene-reinforced dental model resin (GP; G-Print, Graphenano Dental). A DLP-based 3D printer (MAX UV, Asiga) was used to fabricate all casts with a layer thickness of 100 μm .^{4,8} After fabrication, DM casts were ultrasonically cleaned in 98% isopropyl alcohol for 10 minutes (5 minutes of prewash and 5 minutes of postwash).⁴ GP casts were ultrasonically cleaned in 96% ethanol for 5 minutes.²⁹ Thereafter, all casts were left to dry. The GP manufacturer did not suggest a specific polymerization unit to be used with their product; thus, all GP and DM casts were postpolymerized using a xenon polymerization device (OtoFlash G171, NK Optik) under an atmosphere of nitrogen oxide gas for standardization (Fig 1).

Each cast was digitized using the same laboratory scanner to generate test-cast STL (TC-STL) files after storage of one day (T0), 1 week (T1), 2 weeks (T2), 3 weeks (T3), and 4 weeks (T4) in identical light-proof boxes in a room that was temperature-controlled (23°C) by the building's maintenance systems.¹ All STL files were then imported into a metrology-grade 3D analysis software (Geomagic Control X, version 2018.1.1, 3D Systems) indicated by the International Organization for Standardization.³⁰ The software's "region tool" was used to digitally segment the MC-STL into five different regions: anterior (from canine to canine), posterior (right and left

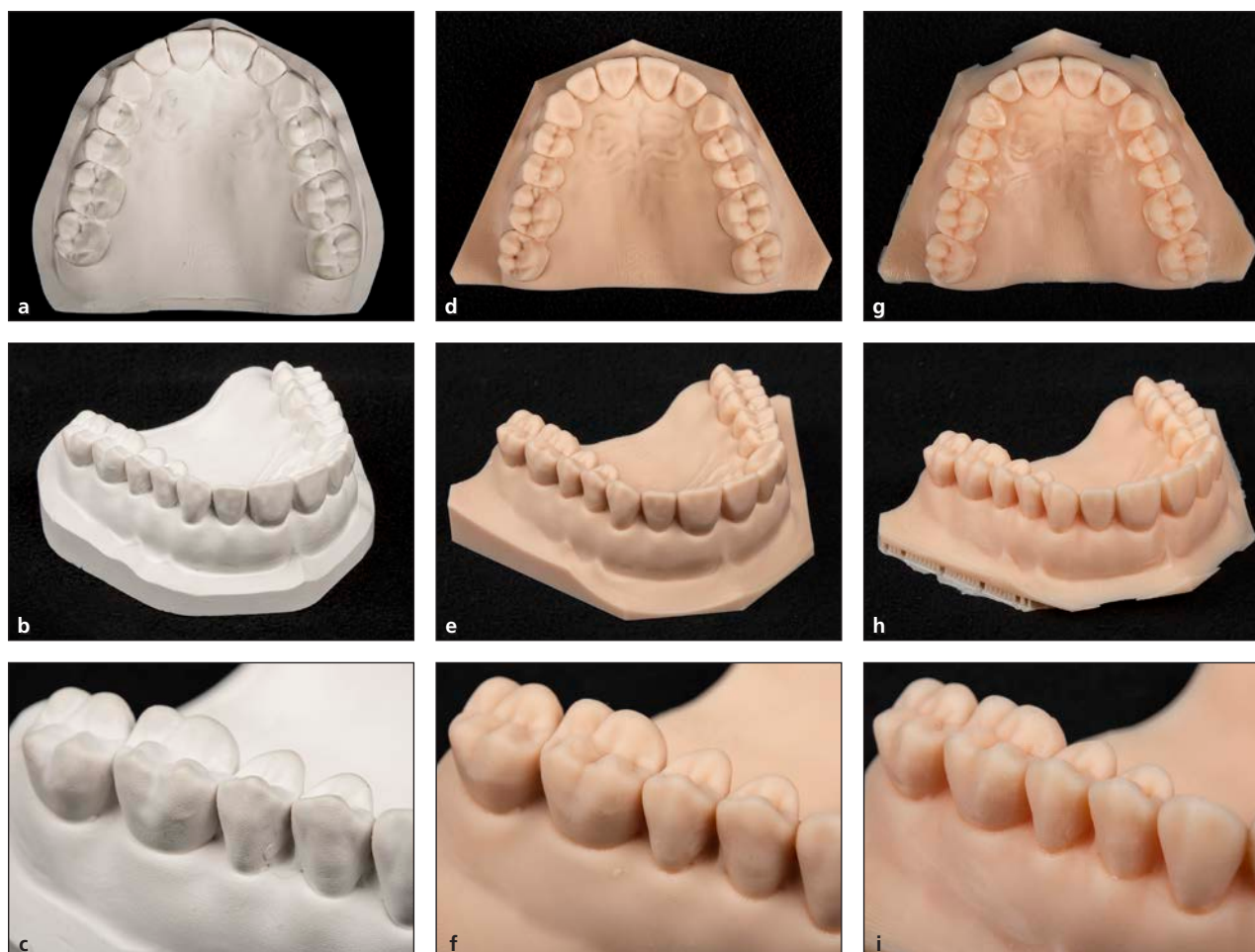


Fig 1 Overview of test groups: (a to c) SC, (d to f) DM, and (g to i) GP.

posterior teeth), entire arch (all teeth), and the entire cast. The software's initial alignment and local best-fit algorithm tools were used to superimpose entire TC-STL data over the MC-STL, which eliminated alignment errors that might arise from different base thicknesses. Color maps of each region were generated for qualitative evaluation, and the deviations at each region were automatically calculated using the root mean square (RMS) method (Figs 2 to 4).

Data normality was verified using Shapiro-Wilk tests. Bonferroni corrected repeated-measures ANOVA tests were used to analyze RMS values at each region, with material type and time interval as main factors. The interaction between the main factors was also included. A statistical analysis software (Jamovi version 2.3.2) was used to perform all analyses ($\alpha = .05$).

RESULTS

Tables 1 to 4 summarize the descriptive statistics of RMS values within each region. The interaction between the

main factors affected the deviations only when anterior deviations were considered ($P < .001$). Material type and time interval had significant effects as main factors when anterior and entire-cast deviations were considered ($P < .001$ for material type; $P \leq .008$ for time interval). Posterior teeth and entire-arch deviations were not affected by the tested parameters ($P \geq .105$).

When clinically relevant pairs (same material or same time interval) were further evaluated for anterior deviations, SC had similar values among different time intervals ($P \geq .601$) and DM had the lowest deviations at T3 ($P \leq .034$). GP had lower deviations at T2 than at other time intervals ($P \leq .041$), except for T3 ($P = .283$). In addition, GP had lower deviations at T3 than at T0 ($P = .011$). Regardless of the time interval, SC had the highest deviations ($P < .001$), while the difference between GP and DM was not significant ($P \geq .090$). T0, T1, and T4 had higher deviations than T3 ($P \leq .027$), whereas every other pairwise comparison resulted in nonsignificant differences ($P \geq .151$).

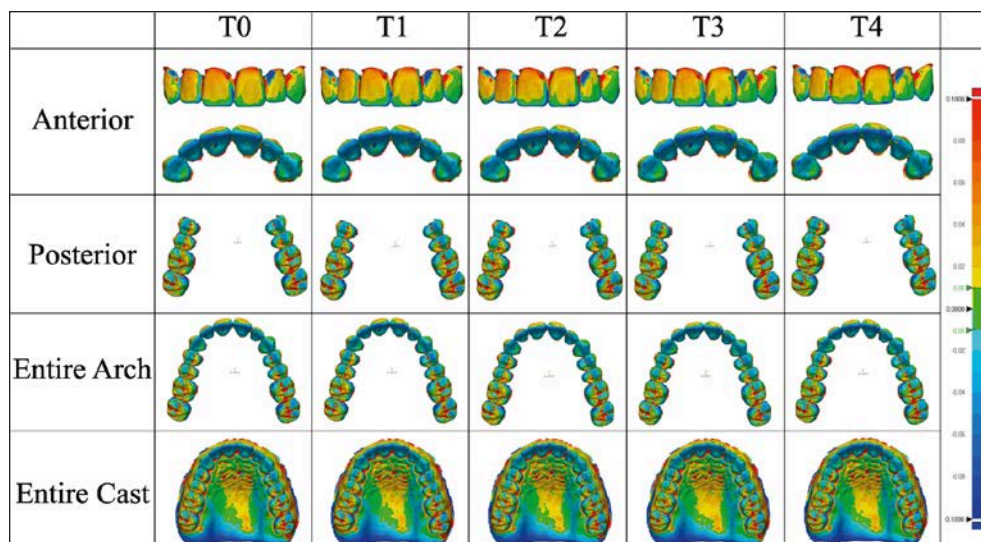


Fig 2 Representative color maps of SCs within each time interval. Red = overcontoured; blue = undercontoured ($\pm 100\text{-}\mu\text{m}$ nominal values); green = acceptable ($\pm 10\text{ }\mu\text{m}$ nominal values).

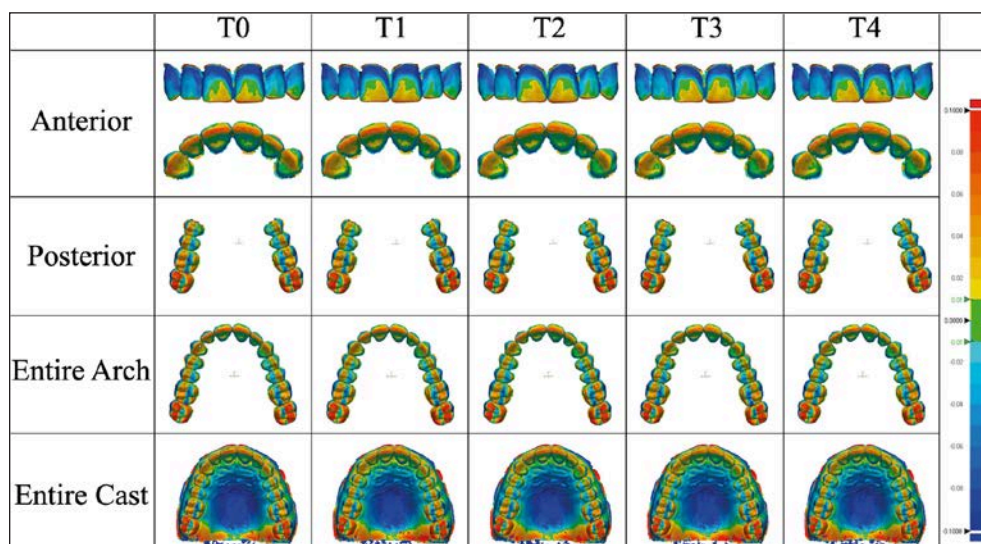


Fig 3 Representative color maps of DM casts within each time interval. Red = overcontoured; blue = undercontoured ($\pm 100\text{-}\mu\text{m}$ nominal values); green = acceptable ($\pm 10\text{ }\mu\text{m}$ nominal values).

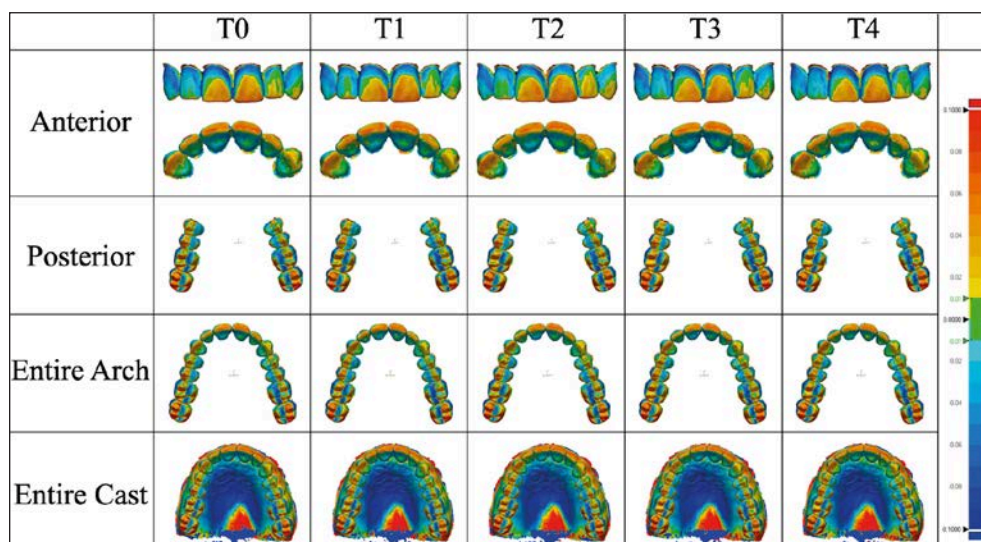


Fig 4 Representative color maps of GP casts within each time interval. Red = overcontoured; blue = undercontoured ($\pm 100\text{-}\mu\text{m}$ nominal values); green = acceptable ($\pm 10\text{ }\mu\text{m}$ nominal values).

**Table 1** Anterior Region Within Each Material–Time Interval Pair

	T0	T1	T2	T3	T4	Total
SC	85.4 ± 11.7 ^{Ba}	85.7 ± 12 ^{Ba}	87.3 ± 12.4 ^{Ba}	85.6 ± 12.4 ^{Ba}	86.4 ± 11.1 ^{Ba}	86.1 ± 11.9*
DM	59.3 ± 5 ^{Ab}	59 ± 5.6 ^{Ab}	58 ± 6.5 ^{Ab}	55.1 ± 5.94 ^{Aa}	58 ± 6.3 ^{Ab}	57.9 ± 5.9 ⁺
GP	52.3 ± 11.4 ^{Ac}	50.9 ± 11.3 ^{Abc}	47.4 ± 11.2 ^{Aa}	49.4 ± 10.4 ^{Aab}	50.8 ± 10.9 ^{Abc}	50.2 ± 11 ⁺
Total	65.7 ± 9.4*	65.2 ± 9.6*	64.2 ± 10.1 ^{**}	63.4 ± 9.6 ⁺	65.1 ± 9.4*	

Data are presented in μm as root mean squares \pm SDs.

Different superscript lowercase letters indicate significant differences in rows, while different superscript uppercase letters indicate significant differences in columns. Different symbols (* and **) indicate significant differences among materials or time intervals. Total values are derived from the pooled data of each material and each time interval ($P < .05$).

Table 2 Posterior Region Within Each Material–Time Interval Pair

	T0	T1	T2	T3	T4	Total
SC	122 ± 45.3	111 ± 19.4	123 ± 45.3	123 ± 46	123 ± 45.3	120.4 ± 40.3
DM	184 ± 188	182 ± 184	180 ± 183	190 ± 192	191 ± 194	185.4 ± 188.2
GP	238 ± 200	238 ± 188	237 ± 191	244 ± 194	243 ± 200	240 ± 194.6
Total	181.3 ± 144.4	177 ± 130.5	180 ± 139.8	185.7 ± 144	185.7 ± 146.4	

Data are presented in μm as root mean squares \pm SDs of both the left and right posterior sections (total of eight teeth).

Table 3 Entire Arch Region Within Each Material–Time Interval Pair

	T0	T1	T2	T3	T4	Total
SC	113 ± 34.6	111 ± 35	111 ± 34.8	112 ± 34.7	113 ± 34	112 ± 34.6
DM	158 ± 146	155 ± 145	153 ± 144	156 ± 150	160 ± 153	156.4 ± 147.6
GP	198 ± 156	196 ± 147	196 ± 150	202 ± 152	201 ± 157	198.6 ± 152.4
Total	156.3 ± 112.2	154 ± 109	153.3 ± 109.6	156.7 ± 112.2	158 ± 114.7	

Data are presented in μm as root mean squares \pm SDs.

Table 4 Entire Cast Within Each Material–Time Interval Pair

	T0	T1	T2	T3	T4	Total
SC	170 ± 44.7	168 ± 44.7	161 ± 37.7	169 ± 42.9	169 ± 43.4	167.4 ± 42.7 ^A
DM	227 ± 111	196 ± 104	199 ± 98.6	231 ± 106	251 ± 109	220.8 ± 107.5 ^A
GP	582 ± 234	554 ± 206	587 ± 211	606 ± 225	581 ± 224	582 ± 220 ^B
Total	326.3 ± 129.9 ^{AB}	306 ± 118.2 ^A	315.7 ± 124.35 ^{AB}	335.3 ± 124.6 ^B	333.7 ± 125.5 ^{AB}	

Data are presented in μm as root mean squares \pm SDs.

Different superscript uppercase letters indicate significant differences among materials and time intervals. Total values are derived from the pooled data of each material and each time interval ($P < .05$).


When entire-cast deviations were considered, GP had the highest values ($P < .001$), and the difference between SC and DM was nonsignificant ($P > .050$). A significant difference among different time intervals was observed between T1 and T3, as higher deviations were observed at T3 ($P = .009$). Every other pairwise comparison among time intervals was nonsignificant ($P \geq .123$).

DISCUSSION

The interaction between the main factors affected the dimensional stability of anterior teeth, while the individual main factors affected the dimensional stability

of anterior teeth and the entire cast. Therefore, the null hypothesis was rejected.

Regardless of the time interval, SC had the highest anterior deviations, and the differences between DM and GP were nonsignificant. The greatest mean difference between SC and the remaining groups was 39.9 μm . However, these differences were the cumulative deviations of anterior teeth, and qualitative interpretation of color maps could be more efficient to speculate on possible clinical outcomes. On the color maps, SC anterior teeth mostly had yellow (slight overcontouring) on the labial surface and varying shades of blue (undercontouring depending on the chroma) on the palatal surface.



For DM, light and dark blue were dominant on most of the labial surface, with evident yellow areas on the middle and incisal thirds of central incisors, while yellow and green were dominant on the palatal surface. In addition, red (overcontouring) was evident on the incisal edges. For GP, the color distribution was similar to that of DM, with magnitudes shifting towards overcontouring on the labial surface. It can be speculated that, while using these casts, esthetics might be affected either over- or undercontouring on labial surfaces and the overcontouring at the incisal edges. Nevertheless, considering that SC had the highest anterior deviations, the labial surface of DM and GP may enable better reproduction of the clinical situation and accurate evaluation of this site. The overcontouring on the palatal surface of DM and GP might cause interferences during static occlusion and affect mounting. The greatest mean difference among time intervals within tested materials was 4.9 μm , which can be considered too small for clinically perception. Therefore, the effect of time interval on the dimensional stability of anterior teeth could be negligible while using the tested materials.

Visible differences were evident in the color maps of posterior teeth and the entire arch, particularly among tested materials. For SC, the occlusal surfaces of posterior teeth were predominantly light blue at the palatal inclination of the buccal cusps and predominantly yellow at the buccal inclination of the palatal cusps, with evident red areas at the central sulcus. Therefore, an adjustment during static occlusion could be required before mounting SC casts, and interferences might be observed during mediotrusive movements. For DM, the second molars had a distinct distribution of red at the palatal inclination of both the buccal and palatal cusps. As for the remaining teeth, yellow was visible at the palatal inclination of the buccal cusps, and blue was visible at the buccal inclination of the palatal cusps. These findings could be interpreted as possible interferences during the static occlusion evaluation due to the second molars and during laterotrusive movements. The color maps of GP were similar to those of DM, but with smaller magnitudes of overcontouring and higher magnitudes of undercontouring at the abovementioned areas. Thus, similar interferences that would require less time to adjust may be expected with GP.

GP had the highest entire-cast deviations, and the greatest mean difference among tested materials was 414.6 μm for the entire cast. This is considerably high, even when the size of the dentate casts is considered. Given that GP had deviations that were either similar to or smaller than those of other materials when dentate areas were considered, the base design may be associated with this result. Color maps also substantiate this hypothesis, as the SC palate was mostly green, while that of DM was light blue and blue. However, the GP palate

was predominantly dark blue, with a distinct red area close to the posterior border. Polymerization shrinkage may be related to undercontouring on both DM and GP palates. The presence of graphene might have disrupted the adhesion of consecutive layers during fabrication or caused a distortion during GP polymerization, which was effective at the initial stages of fabrication. The color distribution of the buccal soft tissue also corroborates this hypothesis, as yellow and green were prominent, regardless of the material. Nevertheless, maxillary GP casts without a palate may be an alternative to SC and DM for diagnostic purposes. The maximum mean difference among time intervals was 29.3 μm , and a difference of this magnitude is rather small for a dentate maxillary model with a palate. Therefore, the time interval's effect on the dimensional stability of entire cast can be considered negligible.

The validity of AM casts was reported in previous studies,^{5,11} with findings similar to the results of the present study. A recent systematic review concluded that the deviations of AM casts ranged between 3.3 and 579 μm .⁹ Only the entire-arch deviations of GP casts were slightly above this range, and tested AM casts may be viable alternatives to evaluate the dentate arch and occlusion, given that the measured deviation values of tested model resins at anterior, posterior, and entire-arch regions were within this range. However, the same systematic review also showed that the acceptable deviation of a cast to be used for prosthetic applications was 200 μm .⁹ Posterior and the entire-arch deviations were either relatively close to or above 200 μm . Therefore, tested model resins should be evaluated for prosthetic purposes.

The present authors are aware of only two previous studies on the dimensional stability of AM dentate casts.^{1,6} In Joda et al's study,¹ AM maxillary casts were stored over a period of 1 month and were evaluated weekly. The authors¹ reported increased deviations after each week, with those after the third and the fourth weeks being significant. The entire cast was also investigated in that study, and the greatest mean difference between time intervals was reported to be 5.6 μm and the greatest mean deviation was reported to be 8.9 μm . Another model resin and model design were used in Joda et al's study, which may influence with these results. The other study⁶ investigated the effect of the 3D printer, storage time, and storage condition on the dimensional stability of AM maxillary casts with palates. Yousef et al⁶ concluded that printer type affected the dimensional stability of casts, and those fabricated with a DLP printer had color changes after 3 months of storage under light exposure.

In the present study, one 3D printer and two model resins were tested, and other printing parameters (such as layer thickness and printing orientation) were not



evaluated. Another limitation was that only one postpolymerization unit was used, and even though the tested polymerization unit has been used in dental studies on deviation analyses,^{4,24} using other units may affect measured deviations, particularly for GP, as the manufacturer did not recommend a polymerization unit. The results were limited to a period of 1 month of storage in light-proof boxes, and longer durations or storage conditions may affect the results. Even though AM casts were fabricated with a solid base and palate (in line with American Board of Orthodontics requirements²⁷) to have a similar shape to that of the stone casts, different base designs or base filling patterns⁹ may affect the dimensional stability. The master cast was digitized 10 times with a high-accuracy IOS³¹ to reflect an actual clinical situation and to eliminate the bias against conventional impressions. Nevertheless, the inherent inaccuracy of IOSs might affect measured deviations, and these results should be substantiated with studies that involve different IOSs. In addition, patient-related factors were not involved in either impression method. Future studies should broaden the findings of the present study with clinical situations that involve edentulous areas, prepared teeth, dental implants, and shorter spans to elaborate upon the limitations of AM casts, particularly those fabricated using tested nanographene-reinforced model resin.

CONCLUSIONS

Within the limitations of this in vitro study, the following conclusions can be drawn:

1. Regardless of the time interval, AM casts had trueness either similar to or higher than that of SCs when dentate regions were considered.
2. Regardless of the time interval, GM casts had large entire-cast deviations, which were primarily sourced from the base and the palate.
3. Dimensional stability of tested casts was high, with a maximum meaningful mean alteration of approximately 29 μm between T0 and T3, when all regions were considered.

ACKNOWLEDGMENTS

The authors report no conflicts of interest.

REFERENCES

1. Joda T, Matthisson L, Zitzmann NU. Impact of aging on the accuracy of 3D-printed dental models: An in vitro investigation. *J Clin Med* 2020;9:1436.
2. Young Kim RJ, Cho SM, Jung WS, Park JM. Trueness and surface characteristics of 3-dimensional printed casts made with different technologies. *J Prosthet Dent* 2023.

3. Zhang ZC, Li PL, Chu FT, Shen G. Influence of the three-dimensional printing technique and printing layer thickness on model accuracy. *J Orofac Orthop* 2019;80:194–204.
4. Yilmaz B, Donmez MB, Kahveci Ç, et al. Effect of printing layer thickness on the trueness and fit of additively manufactured removable dies. *J Prosthet Dent* 2022;128:1318.e1311–e1319.
5. Brown GB, Currier GF, Kadioglu O, Kierl JP. Accuracy of 3-dimensional printed dental models reconstructed from digital intraoral impressions. *Am J Orthod Dentofacial Orthop* 2018;154:733–739.
6. Yousef H, Harris BT, Elathamna EN, Morton D, Lin WS. Effect of additive manufacturing process and storage condition on the dimensional accuracy and stability of 3D-printed dental casts. *J Prosthet Dent* 2022;128:1041–1046.
7. Bohner L, Hanisch M, De Luca Canto G, Mukai E, Sesma N, Neto PT. Accuracy of casts fabricated by digital and conventional implant impressions. *J Oral Implantol* 2019;45:94–99.
8. Tsolakis IA, Papaioannou W, Papadopoulou E, Dalampira M, Tsolakis AI. Comparison in terms of accuracy between DLP and LCD printing technology for dental model printing. *Dent J (Basel)* 2022;10:181.
9. Etemad-Shahidi Y, Qallandar OB, Evenden J, Alifui-Segbaya F, Ahmed KE. Accuracy of 3-dimensionally printed full-arch dental models: A systematic review. *J Clin Med* 2020;9:3357.
10. Reich S, Herstell H, Raith S, Kühne C, Berndt S. In-vitro accuracy of casts for orthodontic purposes obtained by a conventional and by a printer workflow. *PLoS One* 2023;18:e0282840.
11. Aly P, Mohsen C. Comparison of the accuracy of three-dimensional printed casts, digital, and conventional casts: An in vitro study. *Eur J Dent* 2020;14:189–193.
12. Camardella LT, de Vasconcellos Villella O, Breuning H. Accuracy of printed dental models made with 2 prototype technologies and different designs of model bases. *Am J Orthod Dentofacial Orthop* 2017;151:1178–1187.
13. Nestler N, Wesemann C, Spies BC, Beuer F, Bumann A. Dimensional accuracy of extrusion-and photopolymerization-based 3D printers: In vitro study comparing printed casts. *J Prosthet Dent* 2021;125:103–110.
14. Sherman SL, Kadioglu O, Currier GF, Kierl JP, Li J. Accuracy of digital light processing printing of 3-dimensional dental models. *Am J Orthod Dentofacial Orthop* 2020;157:422–428.
15. Maneiro Lojo J, Alonso Pérez-Barquero J, García-Sala Bonmatí F, Agustín-Panadero R, Yilmaz B, Revilla-León M. Influence of print orientation on the accuracy (trueness and precision) of diagnostic casts manufactured with a daylight polymer printer. *J Prosthet Dent* 2023. Epub ahead of print.
16. The G-Print Brochure. Accessed September 20, 2023. https://www.graphenanodental.com/descargas-documentos/diptico-gprint_en.pdf
17. Çakmak G, Donmez MB, Akay C, Abou-Ayash S, Schimmel M, Yilmaz B. Effect of thermal cycling on the flexural strength and hardness of new-generation denture base materials. *J Prosthodont* 2023;32:81–86.
18. Çakmak G, Herren KV, Donmez MB, Kahveci Ç, Schimmel M, Yilmaz B. Effect of coffee thermocycling on the surface roughness and stainability of nanographene-reinforced polymethyl methacrylate used for fixed definitive prostheses. *J Prosthet Dent* 2023;129:507.e501–e506.
19. Agarwalla SV, Malhotra R, Rosa V. Translucency, hardness and strength parameters of PMMA resin containing graphene-like material for CAD/CAM restorations. *J Mech Behav Biomed Mater* 2019;100:103388.
20. Ciocan LT, Ghitman J, Vasilescu VG, Iovu H. Mechanical properties of polymer-based blanks for machined dental restorations. *Materials (Basel)* 2021;14:7293.
21. Di Carlo S, De Angelis F, Brauner E, et al. Flexural strength and elastic modulus evaluation of structures made by conventional PMMA and PMMA reinforced with graphene. *Eur Rev Med Pharmacol Sci* 2020;24:5201–5208.
22. Hernández J, Mora K, Boquete-Castro A, Kina S. The effect of thermocycling on surface microhardness of PMMA doped with graphene: An experimental in vitro study. *J Clin Dent Res* 2020;17:152–161.
23. Ionescu AC, Brambilla E, Pires PM, et al. Physical-chemical and microbiological performances of graphene-doped PMMA for CAD/CAM applications before and after accelerated aging protocols. *Dent Mater* 2022;38:1470–1481.
24. Çakmak G, Rusa AM, Donmez MB, et al. Trueness of crowns fabricated by using additively and subtractively manufactured resin-based CAD-CAM materials. *J Prosthet Dent* 2022.



25. Jin SJ, Kim DY, Kim JH, Kim WC. Accuracy of dental replica models using photopolymer materials in additive manufacturing: In vitro three-dimensional evaluation. *J Prosthodont* 2019;28:e557–e562.
26. Cho SH, Schaefer O, Thompson GA, Guentsch A. Comparison of accuracy and reproducibility of casts made by digital and conventional methods. *J Prosthet Dent* 2015;113:310–315.
27. Rungrojwittayakul O, Kan JY, Shiozaki K, et al. Accuracy of 3D printed models created by two technologies of printers with different designs of model base. *J Prosthodont* 2020;29:124–128.
28. The Sirona website. Accessed September 20, 2023. <https://lp.dentsplysirona.com/content/dam/master/product-procedure-brand-categories/digital-impression/product-categories/intraoral-scanners/ifu/DIM-IFU-Primescan-Connect-EN-6797216-2022-09-12.pdf>
29. The Graphenano website. Accessed September 20, 2023. https://www.graphenanodental.com/descargas-documentos/instrucciones-gprint_en.pdf
30. International Organization of Standardization, ISO 12836. ISO 12836 Dentistry digitizing devices for CAD/CAM systems for indirect dental restorations: Test methods for assessing accuracy. ISO; 2015. <https://www.iso.org/obp/ui/>
31. Mangano F, Lerner H, Margiani B, Solop I, Latuta N, Admakin O. Congruence between meshes and library files of implant scanbodies: an in vitro study comparing five intraoral scanners. *J Clin Med* 2020;9:2174.